Development of a physics-based theory for mixed mode I/II delamination onset in orthotropic laminates

Daneshjoo, Z.; Amaral, L.; Alderliesten, R. C.; Shokrieh, M. M.; Fakoor, M.

DOI
10.1016/j.tafmec.2019.102303

Publication date
2019

Document Version
Final published version

Published in
Theoretical and Applied Fracture Mechanics

Theoretical and Applied Fracture Mechanics 103 (2019) 102303

Contents lists available at ScienceDirect

Theoretical and Applied Fracture Mechanics

journal homepage: www.elsevier.com/locate/tafmec

Development of a physics-based theory for mixed mode I/II delamination onset in orthotropic laminates

Z. Daneshjoo[a,b], L. Amaral[b], R.C. Alderliesten[b,*], M.M. Shokrieh[a], M. Fakoor[c]

[a] Composites Research Laboratory, Center of Excellence in Experimental Solid Mechanics and Dynamics, School of Mechanical Engineering, Iran University of Science and Technology, Tehran 16846-13114, Iran

[b] Structural Integrity & Composites Group, Faculty of Aerospace Engineering, Delft University of Technology, Kluyverweg 1, 2629HS Delft, the Netherlands

[c] Faculty of New Sciences and Technologies, University of Tehran, Tehran 14395-1561, Iran

ARTICLE INFO

Keywords:
Delamination
Laminated composite
Strain energy density
Mixed mode I/II loading

ABSTRACT

This paper demonstrates how the critical strain energy density in the delamination tip vicinity may be used to explain the physics of delamination growth under mixed mode I/II. A theory previously proposed to physically relate mode I and mode II delamination growth is further extended towards describing the onset of mixed mode I/II delamination. Subsequently, data from the literature is used to demonstrate that this new concept of the critical strain energy density approach indeed explains, based on the physics of the problem, the strain energy release rate level at which crack onset occurs. This critical strain energy density for the onset of delamination appears to be independent of the opening mode. This means that, in order to characterize the fracture behaviour of a laminate, fracture tests at only one loading mode are necessary. Because the load level at which the physical delamination onset occurs at the microscopic level is much lower than the traditional engineering definition of macroscopic onset, further work must reveal the relationship between the macroscopically visible delamination onset, and the microscopic onset.

1. Introduction

Laminated fibre reinforced polymer composites are increasingly used in aerospace structures for their high specific strength and stiffness. However, due to the lack of reinforcement in the through-the-thickness direction, these laminated composites are susceptible to delamination, which is the damage mode most often observed in these structures [1,2]. Because delamination has a significant impact on both stiffness and strength, the physics underlying delamination onset and growth must be well understood in order to safely design reliable laminated composite structures.

A substantial amount of papers is available in the literature that presented experimental and/or theoretical studies on delamination growth in composite structures [3–5]. The delamination experiments are generally performed according to available standards [6–9], and the results are presented and evaluated with respect to the fracture toughness, expressed either with the critical strain energy release rate (SERR) from linear elastic fracture mechanics (LEFM), or with the J-integral [10]. Because for various mode mixities, a gradual increase in fracture toughness is observed with the crack extension, often crack growth resistance curves or R-curves are presented that exhibit a steady-state plateau region after an increase from an initiation fracture toughness [11].

When it concerns the pure modes, or the mixed mode in delamination, most studies tend to treat the results phenomenologically, proposing interpolations between the measured fracture toughnesses for various mode mixities, such as the B-K relation [12]. These relations phenomenologically relate a total SERR to the SERR for the pure modes. What these studies illustrate with this approach is the lack of fundamental knowledge of the physics involved in delamination growth [13,14]. Such lack of knowledge of the underlying physics has various drawbacks: it limits the development of more accurate prediction models, and with that it forces the application of large safety margins in design of composite structures [15,16].

In order to shed light on the principles of delamination growth, the present study proposes to examine quasi-static delamination growth with physics-based principles, using the well-known strain energy density (SED) in a novel manner. A first proposal was put forward in a previous publication [13]. Because the SED approach appears not beyond dispute, this proposal has been further studied. As a result, the current paper presents the entire theory for mixed mode I/II loading together with validation of this theory with multiple cases from

* Corresponding author.
E-mail address: R.C.Alderliesten@tudelft.nl (R.C. Alderliesten).

https://doi.org/10.1016/j.tafmec.2019.102303
Received 21 March 2019; Received in revised form 11 June 2019; Accepted 6 July 2019
Available online 08 July 2019
0167-8442/

Nomenclature

ASTM	American society for testing and materials
DCB	double cantilever beam
ENF	end notched flexure
MMB	mixed mode bending
SED	strain energy density
SERR	strain energy release rate
SIF	stress intensity factor
C_{ij}	components of compliance matrix for the plane stress conditions
C'_{ij}	components of compliance matrix for the plane strain conditions
E	Young's moduli of isotropic material
E_i, $i = x, y, z$	Young's moduli of orthotropic material in the i direction
F_I, F_{II}	generalized elastic moduli
G	shear modulus of isotropic material
G_{ij}	shear modulus of orthotropic material in the ij plane
G_I, G_{II}	mode I and mode II strain energy release rate (SERR)
$G_{I_{cr}}$, $G_{II_{cr}}$, $G_{I/II_{cr}}$	critical SERR for the onset of mode I, mode II and mixed mode I/II delamination
$G_{I_{I/II_{cr}}}$, $G_{II_{I/II_{cr}}}$	mode I and mode II components of critical SERR for the onset of mixed mode I/II delamination
$G_{cr}\|_{Exp.}$	critical SERR for the onset of delamination growth obtained via experiments
$G_{cr}\|_{SED}$	critical SERR for the onset of delamination growth calculated using the critical SED approach
K_I, K_{II}	mode I and mode II stress intensity factor (SIF)
$K_{I_{cr}}$, $K_{II_{cr}}$, $K_{I/II_{cr}}$	mode I, mode II and mixed mode I/II fracture toughness
$K_{I_{I/II_{cr}}}$, $K_{II_{I/II_{cr}}}$	mode I and mode II components of critical SIF (fracture toughness) under mixed mode I/II loading
M	mixed mode ratio
r	distance from the crack tip
S	strain energy density factor
S_{cr}	critical strain energy density factor
V	arbitrary volume
W	strain energy
ν	Poisson's ratio of isotropic material
ν_{ij}	Poisson's ratio of orthotropic material in the ij plane
θ	angle from the crack tip
θ_0	crack initiation angle
θ_{0_I}, $\theta_{0_{II}}$, $\theta_{0_{I/II}}$	initial crack growth angle under mode I, mode II and mixed mode I/II loading
φ	mode mixity angle

literature to demonstrate the wide range of validity.

1.1. Background

1.1.1. Connecting micromechanisms and macroscopic damage growth

Indifferent of whether one adopts LEFM through the use of the SERR or whether a J-integral approach is used, the onset of quasi-static delamination growth is determined by the load level just before the crack propagates. This level is then referred to as the fracture toughness for onset of delamination growth [7]. As pointed out in earlier work [17,18], there seems to be a gap between this macroscopic description of delamination through the onset SERR and the micromechanisms acting during the onset of fracture. Several researchers [19–21] have tried to relate the observed microscopic damage features with the macroscopic behaviour of damage growth. Correlating the measured SERRs with the analyses of fracture surfaces then revealed the effects of resin toughness, resin layer thickness and loading mode in the resistance to delamination [22,23]. The results of these studies highlight a difference observed in the resistance to delamination growth under different loading modes. Hibbs and Bradley [19] pointed out that the different micromechanisms acting in delamination growth should connect to the measured fracture toughness for modes I and II. However, they claimed that there must be more to the story. Until recently, a satisfying explanation of the physics connecting delamination growth under different loading modes had not been given.

1.1.2. Connecting mode I, mode II and mixed mode I/II data

In general, the critical SERR, often referred to as fracture toughness, is determined for the pure modes adopting various test standards [7,8]. To predict the delamination growth under mixed mode I/II, many empirical failure criteria have been proposed. An example of mixed mode I/II quasi-static failure criteria is known as the B-K criterion [12]

$$G_{cr} = G_{I_{cr}} + (G_{II_{cr}} - G_{I_{cr}})\left(\frac{G_{II}}{G_I + G_{II}}\right)^{\alpha} \quad (1)$$

Reeder [24] provides an overview on the large amount of state-of-the-art quasi-static failure criteria. He showed that the B-K criterion can be extended to incorporate the transverse shear opening mode III, obtaining a fracture surface criterion (Fig. 1(a)).

Alternative to these analytical relationships, current development of predictive capabilities seems primarily driven by the availability of finite element analysis codes, directing the model development towards the use of cohesive zone formulations [25,26], and more recently XFEM solutions based on these formulations [27,28]. Although generally accepted by the engineering community for providing easy and numerically robust analyses, these cohesive zone formulations, illustrated in Fig. 1(b), are not easily related to the physical fracture mechanisms. What both research approaches have in common is the empirically linking the pure modes through a fitted relationship at the macroscopic level. Despite that these relationships allow for predictions, they do not provide further insight in the underlying physics of these relations.

To address the above-mentioned shortcoming, the work presented in [13] addresses this relationship between microscopic damage features and macroscopic behaviour of damage growth for cracking under modes I and II. In [13], Amaral et al. discuss the use of the strain energy density as a key parameter to understand and relate delamination onset under different opening modes[‡] for a given material. With this, a physics-based relationship between crack growth under modes I and II is presented, and a proposal is made to estimate mode II fracture toughness using only material properties and mode I fracture toughness data. The present study aims at extending the SED concept from [13] further to mixed mode I/II loading, in order to explain the relationship between crack growth at different mode mixities and to obtain mixed mode I/II fracture toughness data from mechanical properties of the material and its mode I fracture toughness.

1.2. Objectives and research questions

This study aims to understand quasi-static crack growth from a physics-based perspective, extending the fundamental relationship that connects mode I and mode II fracture to mixed mode I/II fracture in different materials. This could enable mixed mode I/II fracture data to be obtained from mode I fracture data and material properties. Therefore, the questions addressed in this paper are:

[‡] Although people speak commonly of loading mode, it effectively refers to the crack tip opening mode.

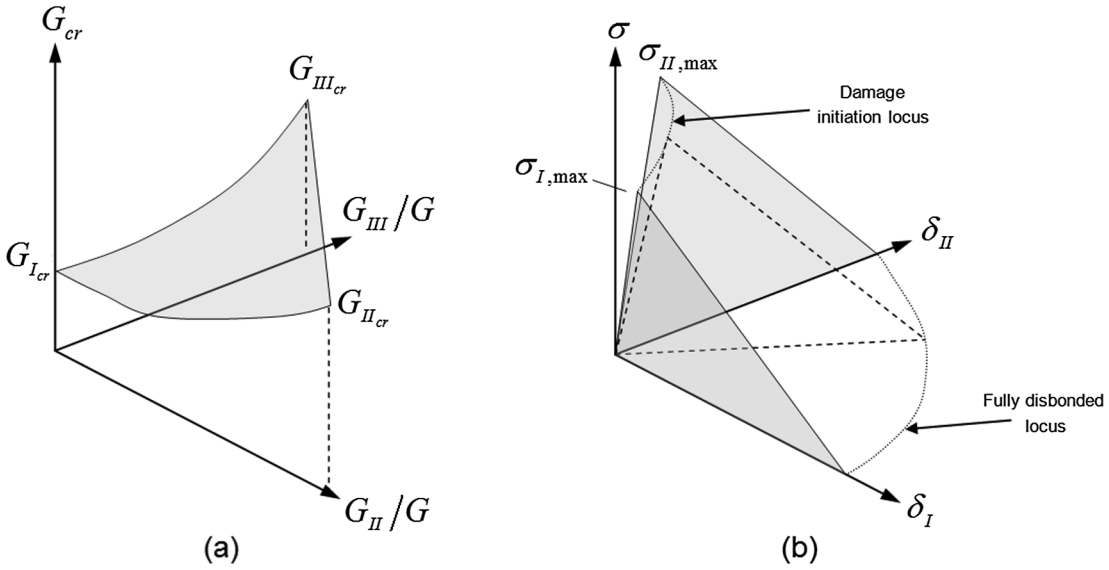

Fig. 1. Schematic of (a) 3D fracture critical surface and (b) mixed-mode I/II cohesive zone model.

- How can the physics-based relationship between mode I and mode II fracture be extended to mixed mode I/II cracking?
- How can one estimate mixed mode I/II fracture toughness from material properties and mode I fracture toughness data?

In order to answer these questions, the present study scrutinizes quasi static delamination growth under mixed mode I/II loading using data available in the literature and correlating these with the SED approach. This is accomplished through an analytical description of the stresses and the strain energy in the vicinity of the crack tip.

2. Hypotheses

For the purpose of clarity, the basic hypotheses of the SED approach and the details of the method, presented in [13], are briefly explained here.

2.1. Fracture and energy

In the current work, the key hypothesis is that all fracture is controlled by energy [29]. Loading a structure implies that potential strain energy is stored in that structure, while onset of fracture occurs for a given material at that point where the strain energy reaches a critical value. This means that fracture is limited by a critical strain energy at which decohesion occurs for that material [30]. That critical strain energy represents then a material property, which implies that the onset of fracture under different opening modes, i.e. shear, tension or combinations thereof, the same energy density is required. Hence, this critical strain energy for the onset of fracture is hypothesized to be independent of the loading mode.

In addition, Neuber [31,32] explained that stresses distributed in the vicinity of the crack tip provide support to the highly stressed area at the tip of the crack. Since the stress distribution ahead of the crack tip, which changes with the loading mode, was shown to determine the damage mechanisms acting on fracture [19], it is postulated here that characterizing the energy dissipated in fracture, requires considering the stress distribution around the crack tip. Physically, this postulation is in agreement with [33–36] in which prediction methods are proposed and validated based on dissipated energy. Taking the critical value of the strain energy density at the onset of fracture, or the corresponding dissipated strain energy as result of that onset fracture effectively relates to the same material characteristic. Although the dissipated energy physically relates to intrinsic fracture resistance of material to specific fracture mechanisms, the specific value at onset might slightly differ, analogue to for example the physics of movement with static and kinetic friction. Hence, to predict onset, the SED is used here, while it

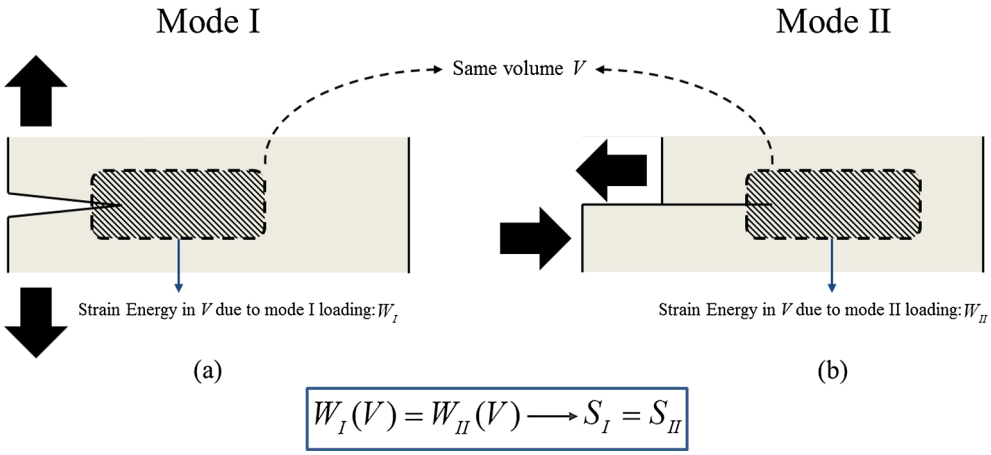

Fig. 2. (a) Cracked body under pure mode I; (b) Cracked body under pure mode II. Both cracked bodies are from the same material. The strain energy density (S) that causes fracture is the same for both loading modes (reproduced from [13]).

will be argued later in the paper, the subsequent process zone development after microscopic onset, might be related to energy dissipation in line with the concepts in [33–36].

2.2. Saint-Venant's principle

Obviously, one has to make a selection of the volume in which these stresses are considered. Here, following the Saint-Venant's principle, i.e. only the strain energy stored in the direct vicinity of the crack tip determines the crack increment, the effect on crack growth of the strain energy stored in areas far away from the crack tip is considered negligible.

However, one has to assume the same arbitrary volume V when evaluating fracture in two cracked bodies of the same material loaded under modes I and II, as illustrated in Fig. 2(a) and (b). The strain energy in this volume V due to mode I loading is $W_I(V)$, while for mode II loading it is $W_{II}(V)$. The critical SED approach hypothesizes that, when the strain energy at a certain point of the body reaches a critical value, the onset of fracture occurs, independently of the loading mode. Mathematically, this can be expressed by equating $W_I(V)$ and $W_{II}(V)$ at the moment of fracture onset. If the volume V at which the strain energy is evaluated for both cases in Fig. 2 is the same, then the critical strain energy per volume that causes the onset of mode I crack growth, S_I, is equal to the critical strain energy per volume that causes the onset of mode II crack growth, S_{II}. This is where the novelty of the present work lies: the amount of energy in the vicinity of the crack tip necessary for the onset of delamination is the same for any loading mode! The reader should note that this hypothesis is different than simply considering that cracks grow when a critical strain energy is reached. Instead, the present study hypothesizes that, not only delamination onset occurs at a given critical SED, but it always occurs at this same critical SED for a given laminate under any loading mode.

2.3. Pure mode I fracture

Relating the critical strain energy density to mode I fracture implies that other dissipation mechanisms are neglected. These mechanisms may relate to friction, contact with load introduction structures, fixture compliance and energy dissipation in the process zone ahead of the main crack tip. These dissipation contributions are regarded to be small for the onset of mode I fracture. Therefore, the stress intensity factor (SIF) and the SERR for the onset of mode I crack growth are considered to include only the effects of energy dissipated in creating a crack length increment.

3. Concept of the strain energy density

Sih [37] has proposed a theory of fracture based on the local strain energy density at the crack tip. This energy density theory forms the basis of the analytical stress/strain solutions developed by Hart-Smith [38] for double lap joints, and is implemented in the computer program A4EI [39], which is used to design and assess various aircraft structures [40] and composite repairs to both composite [41] and metallic airframes [42]. In order to develop the physics-based theory for delamination growth under mixed mode I/II loading, at first, the strain energy density concept is briefly described to provide a general background needed to use it.

3.1. Isotropic materials

For a linear elastic, isotropic material under a general three-dimensional stress field, the strain energy stored in a volume element dV is defined as [43]:

$$dW = \left[\frac{1}{2E}(\sigma_x^2+\sigma_y^2+\sigma_z^2) - \frac{\upsilon}{E}(\sigma_x\sigma_y+\sigma_y\sigma_z+\sigma_z\sigma_x) + \frac{1}{2G}(\tau_{xy}^2+\tau_{xz}^2+\tau_{yz}^2)\right]dV \tag{2}$$

where E is Young's modulus, υ is Poisson's ratio and G is the shear modulus. Assuming that the structure has a through crack that extends on the xy-plane, the stress field around the crack tip is given by [44]

$$\begin{aligned}
\sigma_x &= \frac{K_I}{\sqrt{2\pi r}}\cos(\theta/2)[1-\sin(\theta/2)\sin(3\theta/2)] - \frac{K_{II}}{\sqrt{2\pi r}}\sin(\theta/2)[2+\cos(\theta/2)\cos(3\theta/2)]\\
\sigma_y &= \frac{K_I}{\sqrt{2\pi r}}\cos(\theta/2)[1+\sin(\theta/2)\sin(3\theta/2)] + \frac{K_{II}}{\sqrt{2\pi r}}\sin(\theta/2)\cos(\theta/2)\cos(3\theta/2)\\
\tau_{xy} &= \frac{K_I}{\sqrt{2\pi r}}\cos(\theta/2)\sin(\theta/2)cos(3\theta/2) + \frac{K_{II}}{\sqrt{2\pi r}}\cos(\theta/2)[1-\sin(\theta/2)\sin(3\theta/2)]\\
\sigma_z &= 2\nu\frac{K_I}{\sqrt{2\pi r}}\cos(\theta/2) - 2\nu\frac{K_{II}}{\sqrt{2\pi r}}\sin(\theta/2)
\end{aligned} \tag{3}$$

in which the polar components r and θ are the distance and the angle from the crack tip, K_I and K_{II} are the mode I and II stress intensity factors. The higher order terms of r in Eq. (3) have been ignored. It should be noted that the stress in the z–direction has been considered in this analysis because the crack is locally under plane strain conditions.

Substituting the stresses from Eq. (3) in Eq. (2), we have the following form for the strain energy density:

$$\frac{dW}{dV} = \frac{1}{\pi r}[a_{11}K_I^2 + 2a_{12}K_IK_{II} + a_{22}K_{II}^2] \tag{4}$$

The amplitude or the intensity of the strain energy density field, known as strain energy density factor, S, around the crack tip is defined as [30]:

$$S = a_{11}K_I^2 + 2a_{12}K_IK_{II} + a_{22}K_{II}^2 \tag{5}$$

in which

$$\begin{aligned}
a_{11} &= \frac{1}{16G}[(3-4\nu-\cos\theta)(1+\cos\theta)]\\
a_{12} &= \frac{1}{16G}2sin\theta[\cos\theta-(1-2\nu)]\\
a_{22} &= \frac{1}{16G}[4(1-\nu)(1-\cos\theta)+(1+\cos\theta)(3\cos\theta-1)]
\end{aligned} \tag{6}$$

3.2. Orthotropic materials

Once again, consider a structure with a through crack that extends on the xy-plane is made of a linear elastic, orthotropic material. In this case, the strain energy stored in a volume element dV is given by

$$\frac{dW}{dV} = \frac{1}{2}\left[\frac{\sigma_x^2}{E_x}+\frac{\sigma_y^2}{E_y}+\frac{\sigma_z^2}{E_z}+\frac{\tau_{xy}^2}{G_{xy}}\right] - \frac{\nu_{xy}\sigma_x\sigma_y}{E_x} - \frac{\nu_{xz}\sigma_x\sigma_z}{E_x} - \frac{\nu_{yz}\sigma_y\sigma_z}{E_y} \tag{7}$$

The stresses around the crack tip of an orthotropic cracked body are given by [45]

$$\begin{aligned}
\sigma_x &= \frac{1}{\sqrt{2\pi r}}(K_IA_I(\theta)+K_{II}A_{II}(\theta))\\
\sigma_y &= \frac{1}{\sqrt{2\pi r}}(K_IB_I(\theta)+K_{II}B_{II}(\theta))\\
\tau_{xy} &= \frac{1}{\sqrt{2\pi r}}(K_IC_I(\theta)+K_{II}C_{II}(\theta))\\
\sigma_z &= \frac{1}{\sqrt{2\pi r}}(K_IA_I(\theta)+K_{II}A_{II}(\theta))\frac{\nu_{xz}E_z}{E_x} + \frac{1}{\sqrt{2\pi r}}(K_IB_I(\theta)+K_{II}B_{II}(\theta))\frac{\nu_{yz}E_z}{E_y}
\end{aligned} \tag{8}$$

where the angular functions $A_i(\theta)$, $B_i(\theta)$ and $C_i(\theta)$, for $i = I$ and II, are defined as follows:

$$\begin{aligned}
A_I(\theta) &= Re\left[\frac{x_1x_2(x_2F_2-x_1F_1)}{x_1-x_2}\right],\ A_{II}(\theta) = Re\left[\frac{x_2^2F_2-x_1^2F_1}{x_1-x_2}\right]\\
B_I(\theta) &= Re\left[\frac{x_1F_2-x_2F_1}{x_1-x_2}\right],\ B_{II}(\theta) = Re\left[\frac{F_2-F_1}{x_1-x_2}\right]\\
C_I(\theta) &= Re\left[\frac{x_1x_2(F_1-F_2)}{x_1-x_2}\right],\ C_{II}(\theta) = Re\left[\frac{x_1F_1-x_2F_2}{x_1-x_2}\right]
\end{aligned} \tag{9}$$

where

$$F_1 = \frac{1}{(Cos\theta+x_1Sin\theta)^{\frac{1}{2}}},\quad F_2 = \frac{1}{(Cos\theta+x_2Sin\theta)^{\frac{1}{2}}} \tag{10}$$

x_1 and x_2 are obtained from the conjugate pair of roots of the following characteristic equation.

$$C_{11}x^4 - 2C_{16}x^3 + (2C_{12} + C_{66})x^2 - 2C_{26}x + C_{22} = 0 \tag{11}$$

where the coefficients C_{ij} are obtained from the following stress-strain relationship ($\varepsilon_i = C_{ij}\sigma_j$) [46]:

$$\begin{pmatrix}\varepsilon_x\\ \varepsilon_y\\ \varepsilon_z\\ \gamma_{yz}\\ \gamma_{zx}\\ \gamma_{xy}\end{pmatrix} = \begin{pmatrix} 1/E_x & -\nu_{yx}/E_y & -\nu_{zx}/E_z & 0 & 0 & 0\\ -\nu_{xy}/E_x & 1/E_y & -\nu_{zy}/E_z & 0 & 0 & 0\\ -\nu_{xz}/E_x & -\nu_{yz}/E_y & 1/E_z & 0 & 0 & 0\\ 0 & 0 & 0 & 1/G_{yz} & 0 & 0\\ 0 & 0 & 0 & 0 & 1/G_{zx} & 0\\ 0 & 0 & 0 & 0 & 0 & 1/G_{xy}\end{pmatrix}\begin{pmatrix}\sigma_x\\ \sigma_y\\ \sigma_z\\ \tau_{yz}\\ \tau_{zx}\\ \tau_{xy}\end{pmatrix} \tag{12}$$

Under plane strain conditions, the coefficients C_{ij} should be replaced by C'_{ij} as follows:

$$C'_{ij} = C_{ij} - \frac{C_{i3}C_{j3}}{C_{33}} \tag{13}$$

By substitution of the stresses from Eq. (8) into Eq. (7):

$$\frac{dW}{dV} = \frac{1}{\pi r}[K_I^2 D_1 + K_{II}^2 D_2 + 2K_I K_{II} D_3] \tag{14}$$

Hence, the strain energy density factor, S, is given [45]:

$$S = D_1 K_I^2 + D_2 K_{II}^2 + 2D_3 K_I K_{II} \tag{15}$$

where the coefficients D_1, D_2 and D_3 are given by

$$D_1 = \frac{1}{4}\left[\frac{A_I^2}{E_x} + \frac{B_I^2}{E_y} + \frac{C_I^2}{G_{xy}} - \frac{2A_I B_I \nu_{xy}}{E_x} - \frac{A_I^2\nu_{xz}^2 E_z}{E_x^2} - \frac{B_I^2\nu_{yz}^2 E_z}{E_y^2} - \frac{2A_I B_I \nu_{xz}\nu_{yz}E_z}{E_x E_y}\right]$$

$$D_2 = \frac{1}{4}\left[\frac{A_{II}^2}{E_x} + \frac{B_{II}^2}{E_y} + \frac{C_{II}^2}{G_{xy}} - \frac{2A_{II} B_{II} \nu_{xy}}{E_x} - \frac{A_{II}^2\nu_{xz}^2 E_z}{E_x^2} - \frac{B_{II}^2\nu_{yz}^2 E_z}{E_y^2} - \frac{2A_{II} B_{II} \nu_{xz}\nu_{yz}E_z}{E_x E_y}\right]$$

$$D_3 = \frac{1}{4}\left[\frac{A_I A_{II}}{E_x} + \frac{B_I B_{II}}{E_y} + \frac{C_I C_{II}}{G_{xy}} - \frac{A_I B_{II}\nu_{xy}}{E_x} - \frac{A_{II} B_I \nu_{xy}}{E_x} - \frac{A_I A_{II}\nu_{xz}^2 E_z}{E_x^2} - \frac{B_I B_{II}\nu_{yz}^2 E_z}{E_y^2} - \frac{A_I B_{II}\nu_{xz}\nu_{yz}E_z}{E_x E_y} - \frac{A_{II} B_I \nu_{xz}\nu_{yz}E_z}{E_x E_y}\right] \tag{16}$$

3.3. Strain energy density criterion

According to the SED criterion, the onset of crack growth occurs in the direction θ_0 where the strain energy density factor has its minimum value. Therefore, the angle θ_0 is determined from:

$$\left.\begin{array}{l}\frac{\partial S}{\partial \theta} = 0\\ \frac{\partial^2 S}{\partial \theta^2} > 0\end{array}\right\} \rightarrow \theta = \theta_0 \tag{17}$$

In addition, the onset of crack growth takes place when the value of strain energy density factor along this angle reaches a critical value.

$$S_{\min} = S_{cr} \quad \text{at} \quad \theta = \theta_0 \tag{18}$$

4. Critical strain energy density (SED) approach

4.1. Isotropic materials

Following the discussion in Section 2 of the present study, the critical strain energy density factor, S_{cr}, is independent of loading conditions and crack configuration [30]. So, S_{cr} can be used as a material constant that serves as an indication of the fracture toughness of the material. Therefore, it is reasonable to state that the critical SED necessary for the onset of a pure mode I crack is the same as the critical SED necessary for the onset of mixed mode I/II crack under a certain mixed mode ratio:

$$S_{I_{cr}} = S_{I/II_{cr}} \tag{19}$$

For the case of pure mode I, Eq. (5) takes the simple form:

$$S_I = \frac{K_I^2}{16G}[(3 - 4\nu - \cos\theta)(1 + \cos\theta)] \tag{20}$$

Applying the conditions of Eq. (17) to Eq. (20), it is found that the solution $\theta_{0_I} = 0°$ yields a minimum value for the SED under pure mode I loading. The minimum value of S_I, known as $S_{I_{cr}}$, is, then:

$$S_{I_{cr}} = K_{I_{cr}}^2 \frac{(1 - 2\nu)}{4G} \tag{21}$$

In the presence of both mode I and mode II (mixed mode I/II loading), differentiating S from Eq. (5) with respect to θ and setting $\partial S/\partial\theta = 0$, we have:

$$\frac{\partial a_{11}}{\partial\theta}K_I^2 + 2\frac{\partial a_{12}}{\partial\theta}K_I K_{II} + \frac{\partial a_{22}}{\partial\theta}K_{II}^2 = 0 \tag{22}$$

Inserting the coefficients a_{11}, a_{12} and a_{22} from Eq. (6) into Eq. (22):

$$\frac{K_I^2}{16G}[(\sin\theta.(\cos\theta + 1) + (\sin\theta.(4\nu + \cos\theta - 3)] + \frac{K_I K_{II}}{16G}[4\cos\theta.[\cos\theta - (1 - 2\nu)] - 4\sin^2\theta] + \frac{K_{II}^2}{16G}[\sin\theta.(4 - 4\nu) - sin\theta.(3\cos\theta - 1) - 3\sin\theta.(1 + \cos\theta)] = 0 \tag{23}$$

The mode mixity angle is defined as

$$\varphi = \tan^{-1}\left(\frac{K_{II}}{K_I}\right) \tag{24}$$

which can be range between $\varphi = 0°$ for pure mode I to $\varphi = 90°$ for pure mode II. Inserting K_{II} in terms of K_I and φ from Eq. (24) into Eq. (23) and applying the condition $\partial^2 S/\partial\theta^2 > 0$, the initial crack growth angle θ_0 can be calculated as a function of only Poisson's ratio and mode mixity angle.

$$\theta_{0_{I/II}} = f(\nu, \varphi) \tag{25}$$

Inserting K_{II} in terms of K_I and φ from Eq. (24) into Eq. (5) and substituting $\theta_{0_{I/II}}$ into Eq. (5), the critical strain energy density factor under mixed mode I/II loading is obtained as follows:

$$S_{I/II_{cr}} = \frac{K_{I_{I/II_{cr}}}^2}{16G}[((3 - 4\nu - \cos\theta_{0_{I/II}})(1 + \cos\theta_{0_{I/II}})) + (4sin\theta_{0_{I/II}}(\cos\theta_{0_{I/II}} - (1 - 2\nu))tan\varphi) + ((4(1 - \nu)(1 - \cos\theta_{0_{I/II}}) + (1 + \cos\theta_{0_{I/II}})(3\cos\theta_{0_{I/II}} - 1))\tan^2\varphi)] \tag{26}$$

Applying Eqs. (21) and (26) to the condition in Eq. (19), the mode I and II components of the critical SIF under mixed-mode I/II loading can be determined from the critical mode I SIF, material properties and mode mixity angle as follow:

$$\frac{K_{I_{I/II_{cr}}}}{K_{I_{cr}}} = \left(4(1 - 2\nu)\left[\frac{1}{(3 - 4\nu - \cos\theta_{0_{I/II}})(1 + \cos\theta_{0_{I/II}}) + 4\sin\theta_{0_{I/II}}(\cos\theta_{0_{I/II}} - (1 - 2\nu))\tan\varphi + (4(1 - \nu)(1 - \cos\theta_{0_{I/II}}) + (1 + \cos\theta_{0_{I/II}})(3\cos\theta_{0_{I/II}} - 1))\tan^2\varphi}\right]\right)^{1/2} = g(\nu, \varphi) \tag{27}$$

Therefore,

$$K_{I_{I/II_{cr}}} = K_{I_{cr}}.\, g(\nu, \varphi)$$
$$K_{II_{I/II_{cr}}} = K_{I_{I/II_{cr}}}.\tan\varphi = K_{I_{cr}}.\, g(\nu, \varphi).\tan\varphi \tag{28}$$

where $K_{I_{I/II_{cr}}}$ and $K_{II_{I/II_{cr}}}$ are mode I and II components of the critical SIF in the case of mixed mode I/II loading. It should be noted that Eqs. (27) and (28) are limited to linear elastic, brittle, isotropic materials. This method, which is based on the assumption of Eq. (19), is then referred to as a critical SED approach.

Also, it is noteworthy that in the above equations $\varphi \neq 90°$.

Table 1
Material properties of Plexiglass used for critical SED approach [47].

Poisson's Ratio ν	Shear Modulus G, (GPa)	Mode I Fracture Toughness K_{Icr}, $(MPa.\ m^{1/2})$
0.3447 ± 0.0254	1.151	0.517

In this case as pure mode II, similarly, applying the conditions in Eq. (17) to the simple form of S, $S_{II} = (K_{II}^2/16G).\ [4(1-\nu)(1-\cos\theta) + (1+\cos\theta)(3\cos\theta - 1)]$, the strain energy density factor is shown to achieve a minimum value at $\cos\theta_{oII} = (1-2\nu)/3$ for a linear elastic, isotropic material under pure mode II loading. So, the critical strain energy density factor is

$$S_{II_{cr}} = K_{II_{cr}}^2 \frac{(8(1-\nu) - 4\nu^2)}{48G} \tag{29}$$

The mode II fracture toughness can be determined from mode I fracture toughness and material properties using the condition in Eq. (19) as follows:

$$K_{II_{cr}} = K_{I_{cr}}.\left(\frac{12(1-2\nu)}{(8-8\nu-4\nu^2)}\right)^{1/2} \tag{30}$$

More details of this approach under pure mode II are available in [13].

4.2. Orthotropic composite materials

The calculation of SIF's for composite materials is not straightforward. So, it is better to write the equations in terms of the strain energy release rate. For composite materials under plane strain [46]

$$\begin{aligned} G_I &= F_I K_I^2 \quad (Mode\ I) \\ G_{II} &= F_{II} K_{II}^2 \quad (Mode\ II) \end{aligned} \tag{31}$$

in which

$$\begin{aligned} F_I &= \left[\frac{C'_{11}C'_{22}}{2}\left(\sqrt{\frac{C'_{22}}{C'_{11}}} + \frac{2C'_{12}+C'_{66}}{2C'_{11}}\right)\right]^{1/2} \\ F_{II} &= \left[\frac{C'^2_{11}}{2}\left(\sqrt{\frac{C'_{22}}{C'_{11}}} + \frac{2C'_{12}+C'_{66}}{2C'_{11}}\right)\right]^{1/2} \end{aligned} \tag{32}$$

where the coefficients C'_{11}, C'_{22}, C'_{12} and C'_{66} are obtained from the stress-strain relationships in Eqs. (12) and (13).

Substituting SIF's from Eq. (31) in Eq. (15), the strain energy density factor obtains

$$S = D_1\frac{G_I}{F_I} + D_2\frac{G_{II}}{F_{II}} + 2D_3\left(\frac{G_I G_{II}}{F_I F_{II}}\right)^{1/2} \tag{33}$$

According to the critical SED approach described in detail in the previous section

$$S_{I_{cr}} = S_{I/II_{cr}} \tag{34}$$

Eq. (33) takes the simple form in the case of pure mode I:

$$S_I = D_1\frac{G_I}{F_I} \tag{35}$$

Applying the conditions of Eq. (17) to Eq. (35), it is found that the angle in which the function D_1 reaches its minimum is the angle predicted for the first crack propagation under pure mode I delamination (θ_{0_I}). The strain energy density factor under pure mode I loading has a minimum value in this angle as follows:

$$S_{I_{cr}} = D_1(\theta_{0_I})\frac{G_{I_{cr}}}{F_I} \tag{36}$$

For mixed mode I/II loading, differentiating S from Eq. (33) with respect to θ and setting $\partial S/\partial\theta = 0$

Table 2
Comparison between estimated values of the initial crack growth angle by SED and available experimental values [48] of Plexiglass samples.

Mode Mixity Angle, φ (°)	Initial Crack Growth Angle, $-\theta_{0_{I/II}}$ (°)	
	$-\theta_{0_{I/II}}\|_{SED}$	$-\theta_{0_{I/II}}\|_{Exp.}$
10	17.79	17.38
20	31.97	30.46
30	41.78	42.51
40	49.84	50.87
50	57.08	56.36
60	63.94	62.05
90	80.06	76.50

Table 3
Comparison of mode I and II components of fracture toughness under mixed mode I/II loading predicted by the critical SED approach with the available experimental data [48] of Plexiglass samples.

Mode Mixity Angle, φ (°)	$\left(\frac{K_{I\|I/II_{cr}}}{K_{I_{cr}}}\right)_{SED}$	$\left(\frac{K_{I\|I/II_{cr}}}{K_{I_{cr}}}\right)_{Exp.}$	$\left(\frac{K_{II\|I/II_{cr}}}{K_{I_{cr}}}\right)_{SED}$	$\left(\frac{K_{II\|I/II_{cr}}}{K_{I_{cr}}}\right)_{Exp.}$
10	0.983	1.080	0.173	0.192
20	0.927	1.019	0.337	0.373
30	0.829	0.873	0.479	0.506
45	0.637	0.649	0.637	0.661
60	0.428	0.416	0.741	0.736
75	0.218	0.217	0.814	0.819
80	0.147	0.149	0.835	0.845
90	0.000	0.000	0.874	0.892

Table 4
Material properties of Westerly granite used for critical SED approach [49].

Poisson's Ratio ν	Shear Modulus G, (GPa)	Mode I Fracture Toughness K_{Icr}, (MPa·m$^{1/2}$)
0.21	33.884	2.418

Table 5
Comparison between estimated values of the initial crack growth angle by SED and available. experimental values [49] of Westerly granite samples.

Mode Mixity Angle, φ (°)	Initial Crack Growth Angle, $-\theta_{0_{I/II}}$ (°)	
	$-\theta_{0_{I/II}}\|_{SED}$	$-\theta_{0_{I/II}}\|_{Exp.}$
0	0.00	0.00
34	41.54	42.37
43	47.81	52.64
55.5	56.18	54.03
63	61.19	62.76
72	67.28	65.37
90	77.85	69.23

Table 6
Comparison of mode I and II components of fracture toughness under mixed mode I/II loading predicted by the critical SED approach with the available experimental data [50] of Westerly granite samples.

Mode Mixity Angle, φ (°)	$\left(\frac{K_{I\|I/II_{cr}}}{K_{I_{cr}}}\right)_{SED}$	$\left(\frac{K_{I\|I/II_{cr}}}{K_{I_{cr}}}\right)_{Exp.}$	$\left(\frac{K_{II\|I/II_{cr}}}{K_{I_{cr}}}\right)_{SED}$	$\left(\frac{K_{II\|I/II_{cr}}}{K_{I_{cr}}}\right)_{Exp.}$
0	1.000	0.995	0.000	0.000
26.5	0.885	0.863	0.439	0.428
40	0.755	0.710	0.615	0.598
44	0.697	0.708	0.673	0.685
51.5	0.597	0.603	0.758	0.765
90	0.000	0.000	1.064	1.048

$$\frac{\partial D_1}{\partial\theta}\frac{G_I}{F_I}+\frac{\partial D_2}{\partial\theta}\frac{G_{II}}{F_{II}}+2\frac{\partial D_3}{\partial\theta}\left(\frac{G_I G_{II}}{F_I F_{II}}\right)^{1/2}=0 \tag{37}$$

The mixed mode ratio is defined as

$$\frac{G_{II}}{G}=\frac{G_{II}}{G_I+G_{II}}=M \tag{38}$$

which can be range between $M=0$ (pure mode I) and $M=1$ (pure mode II). Inserting G_{II} in terms of G_I and M from Eq. (38) into Eq. (37) and applying the condition $\partial^2 S/\partial\theta^2>0$, it is found that the angle in which the function D presented below in Eq. (39) reaches its minimum is the angle predicted for the first crack propagation under mixed mode I/II delamination ($\theta_{0_{I/II}}$).

$$D=D_1+\left(\left(\frac{M}{1-M}\right)\left(\frac{F_I}{F_{II}}\right)D_2\right)+\left(2\left(\frac{M}{1-M}\right)^{1/2}\left(\frac{F_I}{F_{II}}\right)^{1/2}D_3\right) \tag{39}$$

So, the initial crack growth angle, $\theta_{0_{I/II}}$, is calculated as a function of material properties and mixed mode ratio

$$\theta_{0_{I/II}}=p(\nu_{ij},\ E_i,\ G_{ij},\ M)\quad i,j=x,y,z \tag{40}$$

Inserting G_{II} in terms of G_I and M from Eq. (38) into Eq. (33) and substituting $\theta_{0_{I/II}}$ into Eq. (33), the critical strain energy density factor under mixed mode I/II loading is

$$S_{I/II_{cr}}=G_{I_{I/II_{cr}}}\left[\frac{D_1(\theta_{0_{I/II}})}{F_I}+\left(\frac{M}{1-M}\right)\frac{D_2(\theta_{0_{I/II}})}{F_{II}}+2\left(\frac{M}{1-M}\right)^{1/2}\left(\frac{1}{F_I F_{II}}\right)^{1/2}D_3\right] \tag{41}$$

Applying Eqs. (36) and (41) to the condition in Eq. (34), the mode I and II components of critical SERR can be determined from mode I critical SERR, material properties and mixed mode ratio as follow

$$\frac{G_{I_{I/II_{cr}}}}{G_{I_{cr}}}=\left(\frac{D_1(\theta_{0_I})}{D_1(\theta_{0_{I/II}})+\left(\frac{M}{1-M}\right)\left(\frac{F_I}{F_{II}}\right)D_2(\theta_{0_{I/II}})+2\left(\frac{M}{1-M}\right)^{1/2}\left(\frac{F_I}{F_{II}}\right)^{1/2}D_3(\theta_{0_{I/II}})}\right)=q(\nu_{ij},\ E_i,\ G_{ij},\ M) \tag{42}$$

Therefore,

$$\begin{aligned}&G_{I_{I/II_{cr}}}=G_{I_{cr}}.\ q(\nu_{ij},\ E_i,\ G_{ij},\ M)\\&G_{II_{I/II_{cr}}}=G_{I_{I/II_{cr}}}.\left(\frac{M}{1-M}\right)=G_{I_{cr}}.\ q(\nu_{ij},\ E_i,\ G_{ij},\ M).\left(\frac{M}{1-M}\right)\rightarrow G_{I/II_{cr}}\\&\qquad=G_{I_{I/II_{cr}}}+G_{II_{I/II_{cr}}}\end{aligned} \tag{43}$$

where $G_{I_{I/II_{cr}}}$ and $G_{II_{I/II_{cr}}}$ are mode I and II components of the critical SERR under mixed mode I/II loading.

It should be noted that in the above equations $M\neq 1$. In this case as pure mode II, similarly, applying the conditions in Eq. (17) to the simple form of S, $S_{II}=D_2(G_{II}/F_{II})$, the strain energy density factor is shown to achieve a minimum value at $\theta_{o_{II}}$ in which the function D_2 reaches its minimum, for a linear elastic, orthotropic material under pure mode II loading. So, the critical strain energy density factor is

$$S_{II_{cr}}=D_2(\theta_{o_{II}}).\left(\frac{G_{II_{cr}}}{F_{II}}\right) \tag{44}$$

The mode II critical SERR can be determined from mode I critical SERR and material properties using the condition in Eq. (34) as

$$G_{II_{cr}}=G_{I_{cr}}.\left(\frac{F_{II}.\ D_1(\theta_{o_I})}{F_I.\ D_2(\theta_{o_{II}})}\right) \tag{45}$$

More details of this approach under pure mode II are available in [13].

Table 7
Material data of unidirectional IM7/8552 carbon/epoxy laminated composite used for critical SED approach [51,52].

E_x (GPa)	$E_y=E_z$ (GPa)	$G_{xy}=G_{xz}$ (GPa)	G_{yz} (GPa)	$\nu_{xy}=\nu_{xz}$	ν_{yz}	$G_{I_{cr}}$ (J/m^2)
165	11.38	5.12	3.92	0.300	0.487	240

Table 8
Estimation of parameters for initial crack growth angle and mixed mode I/II critical SERR predicted by the critical SED approach with comparison of the available experimental data [51] of unidirectional IM7/8552 carbon/epoxy laminated composite.

Mixed mode ratio, M	Angle for minimum D, $-\theta_{0_{I/II}}$ (°)	$G_{I/II_{cr}}\lvert_{SED}$ (J/m^2)	$G_{I/II_{cr}}\lvert_{Exp.}$ (J/m^2)	$\left(\frac{G_{I/II_{cr}}\lvert_{SED}}{G_{I/II_{cr}}\lvert_{Exp.}}\right)$
0.0	34.295	240.000	240	1.00
0.2	41.362	198.799	315	0.63
0.4	48.845	179.075	495	0.36
0.6	55.704	169.915	568	0.30
0.8	63.187	170.160	645	0.26
1.0	80.854	215.770	873	0.25

5. Results and discussion

5.1. Brittle isotropic materials

In this section, in order to evaluate the critical SED approach in mixed mode I/II crack growth of isotropic materials, data from different references in the literature are obtained and the estimated is compared with the available experimental data.

5.1.1. Plexiglass

The first brittle, isotropic, linear elastic material analysed is Plexiglass used by Erdogan et al. [47,48]. The material properties extracted from [47] are given in Table 1.

The values of initial crack growth angle ($\theta_{0_{I/II}}$) in different mode mixity angles (φ) predicted by the critical SED approach are given in Table 2. The validity of these predictions has been checked with the results of the available experiments performed on Plexiglass [48]. The second column gives the theoretical calculations of Eq. (25) based on the critical SED approach and the last column is the average initial crack growth angle of all the measured value obtained from the experiments. As it can be seen the prediction is in a good agreement with the available experimental data.

The comparison between the predictions of Eqs. (27) and (28) via SED and experimental data is shown in Table 3. $(K_{I_{I/II_{cr}}}/K_{I_{cr}})_{SED}$ and $(K_{II_{I/II_{cr}}}/K_{I_{cr}})_{SED}$, shown in column 2 and 4, are the predictions obtained through Eqs. (27) and (28), respectively. $(K_{I_{I/II_{cr}}}/K_{I_{cr}})_{Exp.}$ and $(K_{II_{I/II_{cr}}}/K_{I_{cr}})_{Exp.}$, shown in column 3 and 5, were obtained from experiments described in [48]. It shows the mode I and II components of fracture toughness at any mixed mode ratio can be calculated with good accuracy only using pure mode I fracture toughness and material properties.

5.1.2. Westerly granite

Fracture data from Westerly granite samples were obtained from the literature [49,50] and analysed using the critical SED approach to evaluate the validity of Eqs. (27) and (28) for other brittle materials. The material properties extracted from the literature [49] are listed in Table 4.

Similarly, the results have been shown in Tables 5 and 6.

One can argue that other methods presented in literature predict the onset levels and crack initiation angles equally well. However, one

should keep in mind that these methods make use of empirical relationships against the mode mixity. The results here show that the critical SED approach can predict fracture toughness at a given mode mixity for linear elastic, isotropic, brittle materials, while only needing material properties and mode I fracture toughness. Also, the initial crack growth angle under mixed mode I/II loading can be estimated with the critical SED approach as a function of material properties and mode mixity angle for isotropic materials.

5.2. Orthotropic composite laminates

In the following sections, in order to evaluate the critical SED approach in mixed mode I/II delamination growth of orthotropic composite materials, data from different references in the literature are presented and the theory is compared with the available experimental data.

5.2.1. IM7/8552 carbon/epoxy composite

The first composite material analysed is unidirectional IM7/8552 carbon/epoxy laminated composite used by Williams in [51]. The material data obtained from the literature [51,52] is summarized in Table 7.

The results of solving Eqs. (42) and (43) numerically for the material properties and G_{Icr} given in Table 7 as estimated critical SERR for the onset of mixed mode I/II crack growth, as well as the angles in which the function D is minimum as predicted initial crack growth angle under mixed mode I/II delamination at different mixed mode ratios are shown in Table 8. The accuracy of the estimations is evaluated by comparison with available experimental data [51] given in Table 8.

As it can be seen, increasing the mixed mode ratio i.e., increasing the mode II loading increases the difference between $G_{I/II_{cr}}|_{SED}$ and $G_{I/II_{cr}}|_{Exp.}$ such that the ratio of the critical SERR estimated to the value obtained in mixed mode bending (MMB) experiments performed by Williams [51] starts from approximately 63% for the onset of mixed mode I/II crack growth with $M = 0.2$ to 25% for the onset of pure mode II crack growth. This difference in the critical SERR is attributed to the fact that the value of the critical SERR obtained via MMB experiments does not refer to the onset of crack growth. In the case of mixed mode I/II, the presence of mode II loading develops a fracture process zone by formation of cusps, striations and microcracks ahead of the crack tip. Only when the microcrack coalescence is reached, the crack growth can be observed from the edges of the specimen during MMB tests and the maximum load is used to calculate the value of the critical SERR [22,53]. Hence, mixed mode I/II critical SERR obtained via MMB tests refers to the coalescence of microcracks ahead of the crack tip, but the onset of mixed mode I/II delamination occurs before the specimen reaches its mixed mode I/II critical SERR determined via MMB tests. Additional experiments are needed to verify that this onset indeed happens. This aspect is studied and reported by the authors in another publication [54].

5.2.2. E-glass/vinyl ester composite

The critical SED approach was also applied to unidirectional E-glass/vinyl ester composite whose data is found in [55]. The material data obtained from the literature [55] is given in Table 9.

Similarly, the results have been shown in Table 10.

The results presented in Table 10 show that the onset of mixed mode I/II delamination growth seems to occur from approximately 30% (mixed mode I/II with $M = 0.2$) to 5% (pure mode II) of $G_{I/II_{cr}}|_{Exp}$ for glass/epoxy composite materials. Note that the $G_{I/II_{cr}}|_{SED}$ decreases when the mixed mode ratio increases, while the phenomenological (macroscopic) facture toughness definition always increases with the mixed mode ratio.

Comparing the results of glass/epoxy composite with carbon/epoxy composite, it is found that the value of $(G_{I/II_{cr}}|_{SED}/G_{I/II_{cr}}|_{Exp.})$ depends on number of the microcracks in the fracture process zone before coalescence. Since carbon fibers are stiffer than glass fibers, in glass/epoxy composite materials, the resistance to shear deformation in the resin is smaller. So, the fracture process zone is larger than carbon/epoxy composite materials and coalescence occurs later. Because of this, the values of $(G_{I/II_{cr}}|_{SED}/G_{I/II_{cr}}|_{Exp.})$ for the glass/epoxy composite are smaller than the values for carbon/epoxy composite at a certain mixed mode ratio.

6. Engineering application to mixed mode I/II delamination

The current procedure for characterization of delamination growth under pure mode I, pure mode II and mixed mode I/II involves double cantilever beam (DCB), End notched flexure (ENF) and MMB tests following the ASTM standards [7–9], respectively. Traditionally, delamination onset is defined as the delamination onset visible at a macroscopic level, or an associated point of non-linearity in the load-displacement curve. This macroscopic level of delamination onset is different for the various mode-mixities, and can only be related through an empirical fitted relationship, such as in [12,24]. However, it lacks any physical explanation.

What was demonstrated in this paper is that physically, delamination onset occurs at a microscopic level, at the SERR levels lower than $G_{cr}|_{Exp.}$ obtained via delamination tests. At this microscopic level, the crack onset is visible as a first crack increment under an angle relative to the local mixed mode stresses. The developed theory based on the critical strain energy density, explains both the load level at which this crack onset occurs, as well as the direction in which the crack increment is formed. The theory therefore successfully explains the relation between physical crack onset for any mode mixity in orthotropic laminates. In addition, the theory can be validated by experimental observations as demonstrated here with cases from literature, and in more detail in [13]. An advantage of this theory is that once the physical onset is established with for example quasi-static mode I delamination tests, more complex mode II delamination tests are no longer required, because the critical strain energy density is the same for any opening mode.

According to the results of the critical SED approach for orthotropic composite materials discussed in Section 5.2, it seems a first estimation of $(G_{I/II_{cr}}|_{Exp.})$ is possible by describing the relationship between $G_{I/II_{cr}}|_{SED}$ and $G_{I/II_{cr}}|_{Exp.}$ at a given mode mixity based on the material properties of the composite materials. To this end, the critical SED approach is also applied to other orthotropic composite laminates whose data is found in the literature [51,55–60]. The results are extracted as $(G_{I/II_{cr}}|_{SED}/G_{I/II_{cr}}|_{Exp.})$ at different mixed mode ratios for five carbon/epoxy composites and three glass/epoxy composites. Figs. 3 and 4 indicate the extracted results with a curve fit through them for carbon/epoxy and glass/epoxy composites, respectively. According to Figs. 3 and 4, the value of $(G_{I/II_{cr}}|_{SED}/G_{I/II_{cr}}|_{Exp.})$ is obtained at any arbitrary mixed mode ratio. Since, the value of $G_{I/II_{cr}}|_{SED}$ can be calculated through the critical SED approach (Eqs. (42) and (43)) only having mode I SERR, material properties, the first estimation of $G_{I/II_{cr}}|_{Exp.}$ can be easily obtained without the necessity of performing MMB fracture toughness tests.

What is still required; however, are the relationships between this critical strain energy density and the fracture toughness for the pure modes or mixed mode. The authors believe that now the physical crack

Table 9
Material data of unidirectional E-glass/vinyl ester composite used for critical SED approach [55].

E_x (GPa)	$E_y = E_z$ (GPa)	$G_{xy} = G_{xz}$ (GPa)	G_{yz} (GPa)	$\nu_{xy} = \nu_{xz}$	ν_{yz}	G_{Icr} (J/m^2)
31.10	7.96	3.05	2.76	0.33	0.44	204

Table 10
Estimation of parameters for initial crack growth angle and mixed mode I/II critical SERR predicted by the critical SED approach with comparison of the available experimental data [55] of unidirectional E-glass/vinyl ester composite.

Mixed mode ratio, M	Angle for minimum D, $-\theta_{0_{I/II}}$ (°)	$G_{I/II_{cr}\|SED}$ (J/m^2)	$G_{I/II_{cr}\|Exp.}$ (J/m^2)	$\left(\frac{G_{I/II_{cr}\|SED}}{G_{I/II_{cr}\|Exp.}}\right)$
0.00	32.419	204.000	204.000	1.00
0.33	46.351	175.941	583.866	0.30
0.44	50.300	168.175	1051.005	0.16
0.64	57.367	159.261	1649.788	0.10
0.88	67.552	159.437	2563.200	0.06
1.00	81.270	187.370	3283.000	0.05

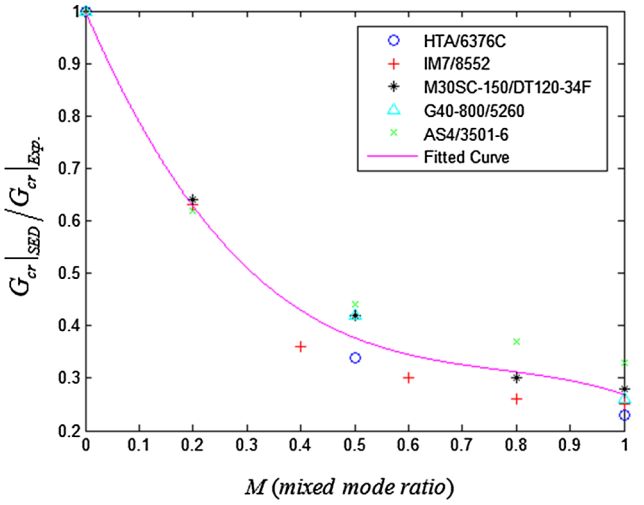

Fig. 3. The extracted $(G_{I/II_{cr}}|_{SED}/G_{I/II_{cr}}|_{Exp.})$ at different mixed mode ratios with a curve fitting for five carbon/epoxy composites.

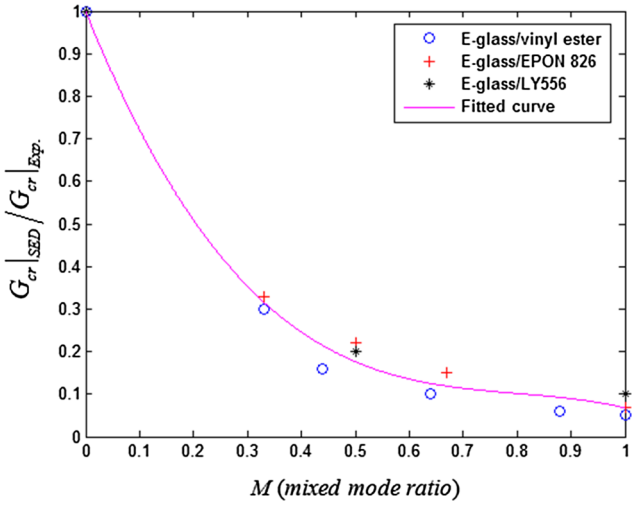

Fig. 4. The extracted $(G_{I/II_{cr}}|_{SED}/G_{I/II_{cr}}|_{Exp.})$ at different mixed mode ratios with a curve fitting for three glass/epoxy composites.

onset is explained, such relationship can be obtained through a similar concept of strain energy dissipation, related to the development of the fracture process zone beyond the physical crack onset. Superimposing this energy dissipation in the fracture process zone development onto the SED component discussed here, will then yield a fully physics based fracture toughness for any mode mixity, settling earlier disputes on the validity of the general SED approach. Additionally, as illustrated with the automated and robotized residual strength characterization in [34], such concept of strain energy density and energy dissipation will enable direct assessment of residual strength of delaminations found in operational aircraft.

7. Conclusion

The current paper presents a theory based on physical principles to explain how physically delamination onset occurs at the crack tip in an orthotropic laminate. The present study demonstrates how the strain energy density reaches a critical level in the crack tip vicinity at the point in which the first onset of crack growth is observed at the microscopic level. This critical strain energy density appears to be independent of the opening mode, and once determined for one opening mode, can be applied to any other mode or combination of modes, having a possible application on reducing the number of fracture toughness tests necessary for understanding quasi-static crack growth in composite structures.

For the engineering practice, where the traditional definition of delamination onset is used, this theory forms a first basis. A relationship between the physical crack onset at the microscopic level and the macroscopic delamination onset is still required and will be the aim of future studies.

Appendix A. Supplementary material

Supplementary data to this article can be found online at https://doi.org/10.1016/j.tafmec.2019.102303.

References

[1] G.S. Amrutharaja, K.Y. Lama, B. Cotterell, Fracture process zone concept and delamination of composite laminates, Theor. Appl. Fract. Mech. 24 (1) (1995) 57–64.
[2] M. Hojo, T. Ando, M. Tanaka, T. Adachi, O. Shojiro, Y. Endo, Modes I and II interlaminar fracture toughness and fatigue delamination of CF/epoxy laminates with self-same epoxy interleaf, Int. J. Fatigue 28 (10) (2006) 1154–1165.
[3] E.S. Greenhalgh, Delamination growth in carbon-fibre composite structures, Compos. Struct. 23 (2) (1993) 165–175.
[4] Z. Daneshjoo, M.M. Shokrieh, M. Fakoor, R.C. Alderliesten, A new mixed mode I/II failure criterion for laminated composites considering fracture process zone, Theor. Appl. Fract. Mech. 98 (2018) 48–58.
[5] M. Kharatzadeh, M.M. Shokrieh, M. Salamat-talab, Effect of interface fiber angle on the mode I delamination growth of plain woven glass fiber-reinforced composites, Theor. Appl. Fract. Mech. 98 (2018) 1–12.
[6] ISO 15024. Fibre-reinforced plastic composites – determination of mode I interlaminar fracture toughness, GIC, for unidirectionally reinforced materials, 2001.
[7] ASTM Standard, D5528 – 13, Standard Test Method for Mode I Interlaminar Fracture Toughness of Unidirectional Fiber-Reinforced Polymer Matrix Composites, ASTM International, US, 2007.
[8] ASTM Standard D7905/D7905M – 14, Standard Test Method for Determination of the Mode II Interlaminar Fracture Toughness of Unidirectional Fiber-Reinforced Polymer Matrix Composites, ASTM International, US, 2014.
[9] ASTM Standard D6671/D6671M − 13e1, Standard Test Method for Mixed Mode I-Mode II Interlaminar Fracture Toughness of Unidirectional Fiber Reinforced Polymer Matrix Composites, ASTM International, US, 2013.
[10] J.R. Rice, A path independent integral and the approximate analysis of strain concentration by notches and cracks, J. Appl. Mech. 35 (2) (1968) 379–386.
[11] Y.W. Mai, Cohesive zone and crack-resistance R-curve of cementitious materials and their fiber-reinforced composites, Eng. Fract. Mech. 69 (2) (2002) 219–234.
[12] M.L. Benzeggagh, M. Kenane, Measurement of mixed-mode delamination fracture toughness of unidirectional glass/epoxy composites with mixed-mode bending apparatus, Compos. Sci. Technol. 56 (4) (1996) 439–449.
[13] L. Amaral, R.C. Alderliesten, R. Benedictus, Towards a physics-based relationship for crack growth under different loading modes, Eng. Fract. Mech. 195 (2018) 222–241.
[14] J.A. Pascoe, R.C. Alderliesten, R. Benedictus, Methods for the prediction of fatigue delamination growth in composites and adhesive bonds – a critical review, Eng. Fract. Mech. 112–113 (2013) 72–96.
[15] R. Jones, A. Kinloch, J. Michopoulos, A.J. Brunner, N. Phan, Delamination growth in polymer-matrix fibre composites and the use of fracture mechanics data for material characterisation and life prediction, Compos. Struct. 180 (2017) 316–333.
[16] R. Jones, S. Stelzer, A.J. Brunner, Mode I, II and mixed mode I/II delamination growth in composites, Compos. Struct. 110 (2014) 317–324.
[17] L. Amaral, L. Yao, R.C. Alderliesten, R. Benedictus, The relation between the strain energy release in fatigue and quasi-static crack growth, Eng. Fract. Mech. 145 (2015) 86–97.

[18] Z. Daneshjoo, M.M. Shokrieh, M. Fakoor, A micromechanical model for prediction of mixed mode I/II delamination of laminated composites considering fiber bridging effects, Theor. Appl. Fract. Mech. 94 (2018) 46–56.
[19] M.F. Hibbs, W.L. Bradley, Correlations between micromechanical failure processes and the delamination toughness of graphite/epoxy systems, ASTM International, West Conshohocken, PA, 1987, pp. 68–97.
[20] A.J. Russell, Micromechanisms of interlaminar fracture and fatigue, Polym. Compos. 8 (5) (1987) 342–351.
[21] W.M. Jordan, W.L. Bradley, Micromechanisms of fracture in toughened graphite-epoxy laminates, ASTM International, West Conshohocken, PA, 1987, pp. 95–114.
[22] C. Corleto, W.L. Bradley, Mode II delamination fracture toughness of unidirectional graphite/epoxy composites, ASTM International, West Conshohocken, PA, 1989, pp. 201–221.
[23] W.L. Bradley, R.N. Cohen, Matrix deformation and fracture in graphite-reinforced epoxies, ASTM International, West Conshohocken, PA, 1985, pp. 389–410.
[24] J.R. Reeder, 3D mixed-mode delamination fracture criteria – an experimentalist's perspective, in: Proceedings of American Society for Composites – 21st Annual Technical Conference, Dearborn, MI; United States, 2006.
[25] C.G. Dávila, C.A. Rose, P.P. Camanho, A procedure for superposing linear cohesive laws to represent multiple damage mechanisms in the fracture of composites, Int. J. Fract. 158 (2) (2009) 211–223.
[26] M.M. Shokrieh, Z. Daneshjoo, M. Fakoor, A modified model for simulation of mode I delamination growth in laminated composite materials, Theor. Appl. Fract. Mech. 82 (2016) 107–116.
[27] L. Zhao, J. Zhi, J. Zhang, Z. Liu, N. Hu, XFEM simulation of delamination in composite laminates, Compos. Part A: Appl. Sci. Manuf. 80 (2016) 61–71.
[28] H. Li, J. Li, H. Yuan, A review of the extended finite element method on macrocrack and microcrack growth simulations, Theor. Appl. Fract. Mech. 97 (2018) 236–249.
[29] A.A. Griffith, The phenomena of rupture and flow in solids, Philos. Trans. Roy. Soc. Lond. Ser. A Contain Papers Math Phys Char 221 (1921) 163–198.
[30] G.C. Sih, Mechanics of Fracture Initiation and Propagation: Surface and Volume Energy Density Applied as Failure Criterion, Springer Science & Business Media, 2012.
[31] H. Neuber, Theory of stress concentration for shear-strained prismatical bodies with arbitrary nonlinear stress-strain law, J. Appl. Mech. 28 (4) (1961) 544–550.
[32] H. Neuber, Theoretical calculation of strength at stress concentration, Czech J. Phys. 19 (3) (1969) 400.
[33] P.W. Mast, G.E. Nash, J.G. Michopoulos, R. Thomas, R. Badaliance, I. Wolock, Characterization of strain-induced damage in composites based on the dissipated energy density Part II. Composite specimens and naval structures, Theor. Appl. Fract. Mech. 22 (2) (1995) 71–96.
[34] J.G. Michopoulos, J. Hermanson, A. Iliopoulos, Advances on the constitutive characterization of composites via multiaxial robotic testing and design optimization, in: J.G. Michopoulos, D.W. Rosen, C.J.J. Paredis, J.M. Vance (Eds.), Advances in Computers and Information in Engineering Research, vol. 1, ASME, New York, 2014, pp. 73–95.
[35] P.W. Mast, L.A. Beaubien, M. Clifford, D.R. Mulville, S.A. Sutton, R.W. Thomas, J. Tirosh, I. Wolock, A semi-automated in-plane loader for materials testing, Exp. Mech. 23 (2) (1983) 236–241. Also published as Failure criteria for composite structures, in High performance composites and adhesives for V/STOL aircraft, NRL Memorandum Report 5231, Naval Research Laboratory, Washington, D.C., 1984, pp. 59–90.
[36] H. Huang, G.S. Springer, R.M. Christensen, Predicting failure in composite laminates using dissipated energy, J. Compos. Mater. 37 (23) (2003) 2073–2099.
[37] G.C. Sih, Strain-energy-density factor applied to mixed mode crack problems, Int. J. Fract. 10 (3) (1974) 305–321.
[38] L.J. Hart-Smith, Adhesive-bonded double-lap joints, NASA Technical Report, NASA-CR-112235, Douglas Aircraft Company, Long Beach, California, 1973.
[39] L.J. Hart-Smith, Design methodology for bonded-bolted composite joints. Vol. II. User manual and computer codes, Technical Report AFWAL-TR-81-3154, 1982.
[40] L. Molent, R.J. Callinan, R. Jones, Design of an all boron epoxy doubler reinforcement for the F-111C wing pivot fitting: structural aspects, Compos. Struct. 11 (1) (1989) 57–83.
[41] CMH-17-3G, Composite Materials Handbook, Volume 3: Polymer matrix composites materials usage, design and analysis, SAE International; Wichita State University, National Institute for Aviation Research, 2012.
[42] R. Jones, D. Hui, Analysis, design and assessment of composite repairs to operational aircraft, in: R. Jones, N. Matthews, A.A. Baker, V. Champagne (Eds.), Chapter 8, Aircraft Sustainment and Repair, Butterworth-Heinemann Press, 2018, pp. 325–456 ISBN 9780081005408.
[43] A.P. Boresi, R.J. Schmidt, O.M. Sidebottom, Advanced Mechanics of Materials, John Wiley, New york, 1993.
[44] G.R. Irwin, Analysis of stresses and strains near the end of a crack traversing a plate, J. Appl. Mech. 24 (1957) 361–364.
[45] G.C. Sih, P.C. Paris, G.R. Irwin, On cracks in rectilinearly anisotropic bodies, Int. J. Fract. Mech. 1 (3) (1965) 189–203.
[46] H. Tada, P.C. Paris, G.R. Irwin, The Stress Analysis of Cracks Handbook, Del Research Corporation, Hellertown, PA, 1973.
[47] F. Erdogan, O. Tuncel, P. Paris, An experimental investigation of the crack tip stress intensity factors in plates under cylindrical bending, J. Basic Eng. 84 (4) (1962) 542–546.
[48] F. Erdogan, G.C. Sih, On the crack extension in plates under plane loading and transverse shear, J. Basic Eng. 85 (4) (1963) 519–527.
[49] C. Wang, Z.M. Zhu, H.J. Liu, On the I-II mixed mode fracture of granite using four-point bend specimen, Fatigue Fract. Eng. Mater. Struct. 39 (10) (2016) 1193–1203.
[50] A.R. Ingraffea, Mixed-mode fracture initiation in Indiana limestone and Westerly granite, The 22nd US Symposium on Rock Mechanics (USRMS), American Rock Mechanics Association, 1981, pp. 186–191.
[51] S.L. Williams Jr., Mixed Mode (I-II) Delamination Fracture Criteria for IM7-G/8552 Intermediate Modulus Carbon/epoxy Composite Laminate, M.Sc. Thesis, North Carolina Agricultural and Technical State University, Greensboro, North Carolina, 2014.
[52] C.Y. Huang, R.S. Trask, L.P. Bond, Characterization and analysis of carbon fibre-reinforced polymer composite laminates with embedded circular vasculature, J. R. Soc. Interface 7 (2010) 1229–1241.
[53] L.E. Asp, A. Sjögren, E.S. Greenhalgh, Delamination growth and thresholds in a carbon/epoxy composite under fatigue loading, J. Compos. Tech. Res. 23 (2) (2001) 55–68.
[54] Z. Daneshjoo, M.M. Shokrieh, M. Fakoor, R.C. Alderliesten, D.S. Zarouchas, Physics of delamination onset in unidirectional composite laminates under mixed-mode I/II loading, Eng. Fract. Mech. 211 (2019) 82–98.
[55] P. Agastra, Mixed Mode Delamination of Glass Fiber/polymer Matrix Composite Materials, M.Sc. Thesis, Montana State University, Bozeman, Montana, 2003.
[56] J.R. Reeder, A bilinear failure criterion for mixed-mode delamination, ASTM International, West Conshohocken, PA, 1993, pp. 303–322.
[57] L. Asp, The effects of moisture and temperature on the interlaminar delamination toughness of a carbon/epoxy composite, Compos. Sci. Technol. 58 (6) (1998) 967–977.
[58] A. Kaddour, M. Hinton, P. Smith, S. Li, Mechanical properties and details of composite laminates for the test cases used in the third world-wide failure exercise, J. Compos. Mater. 47 (20–21) (2013) 2427–2442.
[59] L. Yao, R.C. Alderliesten, M. Zhao, R. Benedictus, Bridging effect on mode I fatigue delamination behavior in composite laminates, Compos. Part A: Appl. Sci. Manuf. 63 (2014) 103–109.
[60] M.M. Shokrieh, A. Zeinedini, S.M. Ghoreishi, On the mixed mode I/II delamination R-curve of E-glass/epoxy laminated composites, Compos. Struct. 171 (2017) 19–31.